Two-mode coupling in a single-ion oscillator via parametric resonance

Dylan J Gorman,[1,*] Philipp Schindler,[1] Sankaranarayanan Selvarajan,[1,2] Nikos Daniilidis,[1] and Hartmut Häffner[1]
[1]*Department of Physics, University of California, Berkeley, California 94720, USA*
[2]*Institut für Experimentalphysik, Universität Innsbruck, A-6020 Innsbruck, Austria*
(Received 21 May 2014; published 27 June 2014)

Atomic ions, confined in radio-frequency Paul ion traps, are a promising candidate to host a future quantum information processor. In this article, we demonstrate a method to couple two motional modes of a single trapped ion, where the coupling mechanism is based on applying electric fields rather than coupling the ion's motion to a light field. This reduces the design constraints on the experimental apparatus considerably. As an application of this mechanism, we cool a motional mode close to its ground state without accessing it optically. As a next step, we apply this technique to measure the mode's heating rate, a crucial parameter determining the trap quality.

DOI: 10.1103/PhysRevA.89.062332 PACS number(s): 37.10.Ty, 03.67.−a

I. INTRODUCTION

The past several decades have yielded tremendous progress in controlling the quantum states of single trapped ions [1–4]. A crucial aspect of experimental work in trapped ion physics is the coupling of the electronic spin to its quantum mechanical motion utilizing transitions at optical frequencies, enabling laser cooling and many body quantum gates. However, the coupling strength of such spin-motion transitions depends crucially on the projection of the laser wave vector onto the mode of interest [3]. Thus, motional modes with small projection onto the laser wave vector remain difficult to control and interrogate, constraining the design of the ion trap as well as the entire experimental apparatus.

In the following, we describe a parametric coupling scheme allowing experimental access to any vibrational mode of a single ion without direct optical interaction, provided there is optical access to any single mode.

For this, an oscillating potential is applied to trap electrodes such that the associated field features a spatial variation enabling the coupling. We consider this first in the case of a general two-dimensional harmonic oscillator with the potential $\frac{m}{2}(\omega_x^2 x^2 + \omega_y^2 y^2)$. The introduction of a perturbing potential with a term proportional to xy will make the instantaneous eigenmodes of the system no longer align purely in the x and y directions, creating a coupling between the modes. If the two modes have different frequencies, energy conservation considerations imply that single quanta cannot be exchanged between the two modes if the coupling potential is static in time. This exchange becomes possible by modulating the perturbing potential. The energy difference between the two modes is then made up for by either absorbing a quantum from, or emitting a quantum into, the driving field. This system features dynamics where the motional energy oscillates between the mode aligned with the x axis (the X mode) and the one aligned with the y axis (the Y mode).

In Paul traps, the ion is effectively confined in a three-dimensional oscillator potential, which arises by applying radio-frequency (rf) and static voltages to a number of trap electrodes. The trapped ion's motion can be decomposed into three normal modes. In order to couple two of the normal modes, we add a time-varying voltage to one or more nearby electrodes, which oscillates at the difference between the modes' frequencies.

A similar method of mode-mode coupling was proposed and demonstrated for charged particles in Penning traps [5–7] where the axial and cyclotron modes of a single charged particle are coupled by an additional electric field. We apply these methods to microfabricated surface traps, which are a promising candidate for a scalable quantum information processor [8] but have inherently limited optical access. For example, a mode orthogonal to the plane of the trap may be optically inaccessible to avoid exposure of trap electrodes to laser light. Trap geometry or vacuum chamber design may impose further constraints on optical access. We demonstrate that this technique can be used to cool trap modes lacking substantial overlap with the wave vector close to their ground state and directly apply this technique to perform a heating rate measurement without directly accessing the mode of interest. Thus, this scheme allows an experimenter to manipulate all motional modes of a single ion, even when optical access is restricted.

This paper is organized as follows. In Sec. II we discuss the theory of this interaction. Section III covers the details of our experiment and characterizes the coupling process in the frequency domain. Section IV includes our experimental results, where we show several applications of this technique. Finally, Sec. V summarizes our results and suggests extensions to this work.

II. THE COUPLING MECHANISM

We consider an ion, with charge q and mass m, confined in a linear surface electrode rf Paul trap. In such a trap, an oscillating voltage with frequency in the range of $2\pi \times 30$ MHz will be applied to two electrodes (labeled "RF" in Fig. 1) providing two-dimensional confinement along the x and y axes. In general, the motion of an ion in such a trap is a solution to the Matthieu equation [9], but usually the dynamic trapping effects can be neglected in favor of the "pseudopotential approximation" [10]. In this approximation, the time-dependent Hamiltonian induced by the trapping rf is replaced with a time-independent harmonic oscillator with motional frequencies ω_x and ω_y. In our case the rf pseudopotential generates no confinement in a third direction,

*dgorman@berkeley.edu

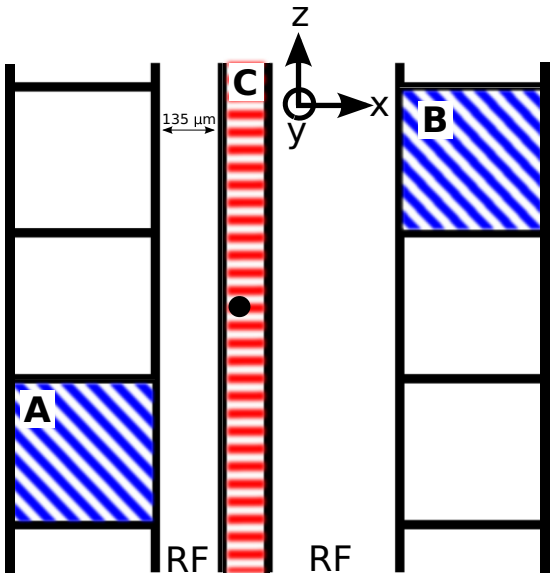

FIG. 1. (Color online) Illustration of the surface trap where the ion's position is represented by the black dot. When the experiment is operated in the xz coupling configuration, the rf parametric drive is applied to the electrodes labeled A and B (blue diagonal shading). When operated in the xy coupling configuration, the drive is applied to the electrode labeled C (red horizontal shading).

z. The confinement in the z direction is the result of a dc potential which is quadratically varying in space, giving the ion a third motional frequency, ω_z. The total Hamiltonian is then treated as the pseudopotential from the trapping rf field, plus the total electrostatic potential. In the following, we consider the trapping potential static, and the only time varying field is the one enabling the mode-mode coupling.

Working in the aforementioned approximation, we consider a harmonically confined ion with motional frequencies ω_i, $i \in \{x,y,z\}$. The interaction energy created when a voltage V is applied to a nearby coupling electrode is $qU(\mathbf{r})V$. $U(\mathbf{r})$ is the potential per volt applied to the electrode, describing the spatial profile of the potential at the trapping position due to the coupling electrode. To enable the mode-mode coupling, we modulate the voltage on a set of electrodes whose spatial profile mixes two of the ion's normal vibrational modes.

Then the Hamiltonian governing the motion is $H = H_{\rm osc} + qU(\mathbf{r})V$, with $H_{\rm osc} = \hbar \sum_i \omega_i a_i^\dagger a_i$ being the harmonic oscillator Hamiltonian and a_i ($a_i^\dagger$) being the annihilation (creation) operator for mode i. To achieve mode-mode coupling, we apply an oscillating rf voltage on a judiciously chosen set of coupling electrodes such that $V = V_0 \cos(\omega_p t)$. If $\omega_p = \omega_i - \omega_j$, the difference frequency between modes i and j, a parametric coupling emerges in the Hamiltonian.

To see the coupling explicitly, the spatial profile $U(\mathbf{r})$ is expanded to second order as $U(\mathbf{r}) = U(0) + \sum_i (r_i/C_i) + (1/2)\sum_{i,j}(\pm)(r_i r_j)/D_{ij}^2$. C_i and D_{ij}^2 are the inverses of the coefficients in a Taylor expansion of the spatial profile around the trapping region. The linear terms create an electric field at the ion position and present a driving force on the ion which introduces a driven motion analogous to micromotion. As we show later, this additional term does not alter the coupling dynamics and thus can be neglected if the set of coupling electrodes is chosen such that the coupling dominates over this driving force.

The terms proportional to r_i^2 modify the motional frequencies of the ion. If the modulation frequency is near the resonance condition $\omega_p \approx 2\omega_i$, these terms effect a parametric amplification of the energy in the ω_i mode [11]. However, if ω_p is far from this condition (as is the case in our experiments), the modulation of the trap frequency contributes only an overall phase to the ion's spatial wave function. Finally, the cross terms proportional to $r_i r_j$ are responsible for the parametric coupling with the drive frequency chosen appropriately.

In the interaction picture, the Hamiltonian becomes

$$\begin{aligned} H_I &= qV_0 \cos(\omega_p t) \sum_{i,j} \left(\frac{r_i r_j}{2D_{ij}^2} \right) = qV_0 \hbar \cos(\omega_p t) \\ &\quad \times \sum_{ij} \frac{e^{i(\omega_i+\omega_j)t} a_i^\dagger a_j^\dagger + e^{i(\omega_i-\omega_j)t} a_i^\dagger a_j + \text{H.c.}}{4m\sqrt{\omega_i \omega_j} D_{ij}^2} \\ &= \hbar \cos(\omega_p t) \sum_{ij} g_{ij} (e^{i(\omega_i+\omega_j)t} a_i^\dagger a_j^\dagger \\ &\quad + e^{i(\omega_i-\omega_j)t} a_i^\dagger a_j + \text{H.c.}), \end{aligned} \tag{1}$$

where H.c. indicates Hermitian conjugation. Here, the sum is taken over the coordinate axes $i \in \{x,y,z\}$. In the last line we have absorbed all the constants except $\hbar$ into the coupling frequency g_{ij}. In general, we expect the rotating wave approximation (RWA) to be valid whenever $g_{ij} \ll \omega_{i,j}$.

If $\omega_p = \omega_i - \omega_j$ and applying the RWA, all the terms in the sum of Eq. (1) vanish except the one involving coupling oscillators i and j leading to

$$H_I \approx \hbar g_{ij} (a_i a_j^\dagger + a_i^\dagger a_j). \tag{2}$$

This is precisely the interaction we have sought to create: it will swap the quantum states between oscillator modes i and j at the frequency g_{ij}. By applying the parametric drive for a specific duration, we can controllably induce state swapping between any two modes of the single ion oscillator.

When the parametric drive is operated on resonance, that is, $\omega_p = \omega_i - \omega_j$, the interaction picture Hamiltonian is diagonal in the basis of two modified normal modes given by $\frac{1}{\sqrt{2}}(a_i \pm a_j)$. The modes are split in frequency by $2g_{ij}$. If the drive is detuned by Δ from the parametric resonance, the form of the interaction picture Hamiltonian changes. To treat this problem, it is easiest to transform to a particular interaction picture in which

$$H_I \approx \hbar \frac{\Delta}{2} (a_i^\dagger a_i - a_j^\dagger a_j) + \hbar g_{ij} (a_i a_j^\dagger + a_i^\dagger a_j). \tag{3}$$

The eigenvalue splitting of this Hamiltonian is given by $2\sqrt{g_{ij}^2 + 4\Delta^2}$. Thus, optical spectroscopy of the ion motion will show the bare resonance at ω_i split into two lines as the parametric drive is operated near resonance. Varying both laser frequency and the parametric drive detuning will show a familiar avoided crossing behavior, providing a witness of the parametric interaction.

In addition to driving the system at the difference frequency between the two modes, one can also drive the system at the

sum frequency. In that case, Eq. (1) becomes

$$H_I \approx \hbar g_{ij}(a_i^\dagger a_j^\dagger + a_i a_j) \tag{4}$$

in the RWA. This means that the system can be operated as a parametric amplifier if it is driven by the sum frequency of the two modes.

III. EXPERIMENTAL IMPLEMENTATION

In our experiment, a single $^{40}Ca^+$ ion is trapped about 100 μm above the surface of a microfabricated surface-electrode rf Paul trap, where sideband cooling and analysis of the motional state are performed on the metastable $4\,^2S_{1/2} \leftrightarrow 3\,^2D_{5/2}$ transition. The ion has three motional modes, with axes nearly parallel to the Cartesian axes defined in Fig. 1. The motional frequencies along these three axes are about $(\omega_x,\omega_y,\omega_z) \approx 2\pi \times (2.6\ \text{MHz}, 2.9\ \text{MHz}, 1.0\ \text{MHz})$. Doppler cooling, sideband cooling, and state manipulation are accomplished with lasers in the x-z plane, with about 45° projection onto both the x and z axes. The angle of the laser wave vectors onto the y axis is 9°, making the Y motional mode difficult to analyze directly. Doppler cooling prepares the X (Z) modes to a mean occupation of ≈6 (20) motional quanta, and sideband cooling reduces these values to less than 0.3 quanta in either mode. Owing to small coupling of the Doppler cooling laser onto the Y mode, its occupation is of the order of 20 quanta after Doppler cooling despite this mode having nearly the same frequency as the X mode. For similar reasons, sideband cooling is not feasible at all on the Y mode.

Depending on which modes ought to be coupled, the field needs to be applied to a set of electrodes maximizing the coupling term while keeping the linear terms sufficiently small. Throughout this article we use two configurations that couple either the X and Y modes or the X and Z modes. For the first (xy) configuration we simply apply the coupling field to the electrode marked C in Fig 1. In the case of the xz configuration, driving a single electrode is not sufficient as it would result in excessive driving force on the ion [details in Sec. III A]. Therefore, we aim to apply voltages with a ratio of 1:4 to electrodes A and B, which constitutes the optimal configuration when being constrained to driving two electrodes in phase. This ratio arises because electrode B is farther from the ion than electrode A and represents the condition in which the total driving field on the ion in the z direction is zero.

Each experiment begins with with Doppler cooling on the $4\,^2S_{1/2} \leftrightarrow 4\,^2P_{1/2}$ transition and optical pumping into the $m_s = -1/2$ state, followed by a fixed length coherent excitation pulse and electron shelving state readout [12,13]. Spectroscopy is carried out on the $|L,m_J\rangle = |S,-1/2\rangle \rightarrow |D,-1/2\rangle$ transition. The state of the motional mode i is probed by evaluating the strength of the sidebands of this transition detuned by $\pm\omega_i$ [14].

The parametric interaction is studied in two ways. It is first characterized by operating it in *continuous-wave* (CW) mode. In this mode, the drive is active throughout the experiments and the spectroscopic signatures of coupling are observed. It is also operated in *pulsed mode* where the coupling field is switched on for a fixed time after the initial state preparation giving access to the time dynamics of the coupling process.

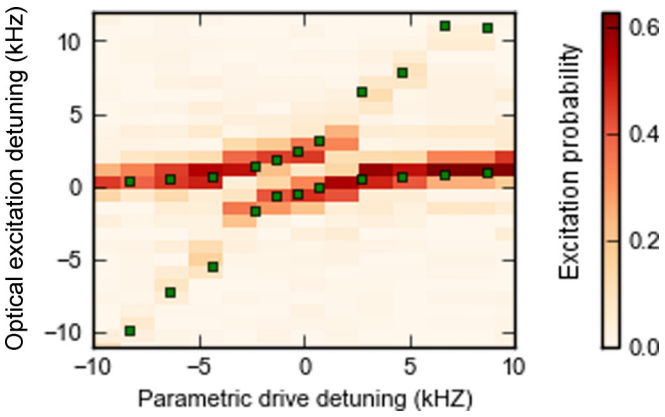

FIG. 2. (Color online) Measured energy spectrum of the X radial sideband illustrating the avoided crossing as a function of the detuning of the parametric drive operated in the xy coupling configuration. The spectrum would look qualitatively identical in the xz configuration. The green squares represent the mean values of Lorentzian fits to determine the frequency splitting.

A. Characterization of the parametric drive interaction

The experimentally simplest way to investigate the parametric interaction is to first operate it in CW mode near the parametric resonance condition. Then, laser spectroscopy near one of the secular sidebands (indexed by i or j) will show two Lorentzian line shapes split in frequency space by $2\sqrt{g_{ij}^2 + 4\Delta^2}$, where Δ is the detuning of the parametric drive from the resonance condition.

By measuring the spectrum around the sideband transition for several drive frequencies ω_p, the precise resonance frequency and the coupling strength can be determined from the avoided crossing as shown in Fig. 2. At parametric resonance, the line splitting features a minimum, and the coupling strength equals half the on-resonance splitting. In our setup, coupling strength is limited by the maximum voltage that can be applied to the coupling electrodes, which are heavily filtered by in-vacuum low-pass filters to suppress heating from technical noise sources [15]. Nevertheless, we have been able to achieve coupling frequencies approaching $2\pi \times 10$ kHz for both xz and xy coupling configurations.

This coupling frequency should be compared to the amplitude of the driven motion due to the electric field component of the parametric drive. The presence of an electric field at the trapping position due to the parametric drive causes a force on the atom which can be characterized and managed in a fairly straightforward way.

The driven motion amplitude may be quantified by operating the parametric drive in a CW mode. Then, the oscillating electric field at the ion position results in driven motion, analogous to the well-known micromotion [12]. This driven motion causes the ion to experience a frequency-modulated laser field, redistributing the laser power in frequency space and reducing the laser power at the resonant frequency. This effect gives rise to sidebands around the laser's carrier frequency at integer multiples of the driven motion frequency. For a CW coupling field, the effect is completely analogous to micromotion leading to a reduced coupling strength on the resonant optical transition which can be observed by a decrease

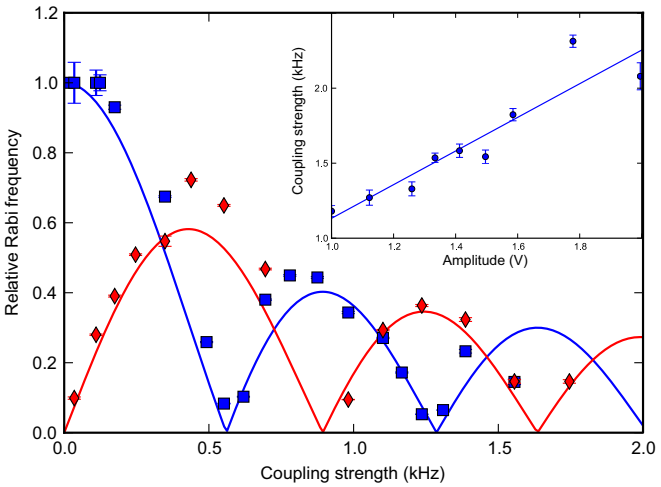

FIG. 3. (Color online) Relative Rabi frequency on the carrier (blue squares) and driven motion sideband (red diamonds), compared to the unperturbed Rabi frequency on the unperturbed carrier, as a function of parametric coupling strength in the xz coupling configuration. The solid lines represent fitted Bessel functions of the first kind. The inset illustrates the parametric coupling strength g_{xz} as a function of drive voltage amplitude prior to the in-vacuum low-pass filters.

in the Rabi frequency Ω_c. As in the case of micromotion, the optical transition can be driven by detuning the laser by an integer multiple n of the driving electric field frequency. In that case, the transition strength is given by [16]

$$\Omega_c \rightarrow |J_n(kA)|\Omega_c \tag{5}$$

for a given oscillation amplitude A along the laser propagation direction $\vec{k}$, with J_n being the nth order Bessel function of the first kind. We note that if the laser is not detuned, i.e., is on resonance with the optical transition, the coupling strength is reduced by $J_0(kA)$.

To measure this effect, we apply a continuous drive (off-resonant from all the motional modes and first-order parametric resonances) onto the coupling electrodes and measure the frequency of Rabi oscillations on the $|L,m_J\rangle = |S,-1/2\rangle \rightarrow |D,-1/2\rangle$ transition. From this, we can extract the driven motion amplitude as a function of the parametric drive amplitude from Eq. (5). Figure 3 shows the normalized Rabi frequencies on the carrier and the driven motion sideband as a function of the coupling strength for the xz coupling configuration where $\omega_p = 2\pi \times 1.7$ MHz. This allows us to determine the driven motion amplitude as a function of the coupling strength to be

$$A = \frac{497(8)\text{ nm}}{(2\pi \times 1\text{ kHz})} g_{xz}. \tag{6}$$

In the xy configuration, the drive is applied to an electrode directly beneath the ion so that most of the driven motion is in the direction orthogonal to the laser and therefore does not significantly affect the optical coupling strength.

B. Pulsed mode operation of the drive

In the remainder of this work, we investigate parametric coupling in the pulsed mode. If the parametric drive is switched on and off rapidly, the micromotion analogy of Eq. (5) no longer holds, and the unwanted electric field can induce considerable off-resonant excitation in the oscillator modes, disturbing the coupling dynamics. However, this electric field contribution to the total Hamiltonian has no notable influence on the coupling dynamics if it is switched on and off slowly enough, i.e., it is adiabatic. Here, the criterion for adiabaticity is to avoid off-resonant excitation of the oscillator mode itself. Experimentally, we shape the coupling field strength with a Blackman windowing function, which has proven to effectively reduce off-resonant excitation in a two-level system [17,18]. More precisely, the window for a pulse with duration T is described by

$$B_T(t) = \frac{1-\alpha}{2} - \frac{1}{2}\cos\left(2\pi\frac{t}{T}\right) + \frac{\alpha}{2}\cos\left(4\pi\frac{t}{T}\right),$$

where $\alpha = 0.16$. In order to facilitate the comparison to rectangular pulses, the coupling duration of a Blackman-shaped pulse B_T is defined as the duration of a rectangular pulse T_{rect} with the same pulse area so that $T = T_{\text{rect}}/0.42$. Experimentally, using these pulses for the xz configuration reduces the off-resonant excitation to less than 0.3 quanta for a reasonable coupling strength of several kHz.

C. Population swapping

The first analysis in the pulsed mode is to demonstrate that the population can be exchanged between two motional modes. This serves as an experimental definition of the exchange operation (SWAP) and forms the cornerstone for the cooling and analysis techniques presented later. To facilitate optical analysis of both the involved motional modes, we focus here on population swapping in the xz configuration, but note that one can construct a SWAP operation between any two modes and show as an example swapping in the xy configuration.

To demonstrate population swapping, a single mode was sideband cooled close to its ground state. For the xz configuration, the Z mode was cooled, and for the xy configuration, the X mode was cooled, followed by a mode coupling pulse, applied for a variable time. The motional state after the coupling was probed on the red sideband of either mode on the $|S,-1/2\rangle \rightarrow |D,-1/2\rangle$ transition. As the mean phonon number in a given mode drops significantly below one, the excitation probability is suppressed [3,12]. The dynamics of the coupled systems are illustrated in Fig. 4 where the periodic oscillations of the excitation probability represent a hallmark feature of the coupling. This furthermore allows us to define a SWAP operation where the states of the two modes are completely exchanged at around 90 μs for xz coupling and at around 50 μs for xy coupling. For the xz coupling configuration, a Blackman-shaped pulse needs to be used whereas for the xy configuration a square pulse is sufficient to suppress off-resonant excitation.

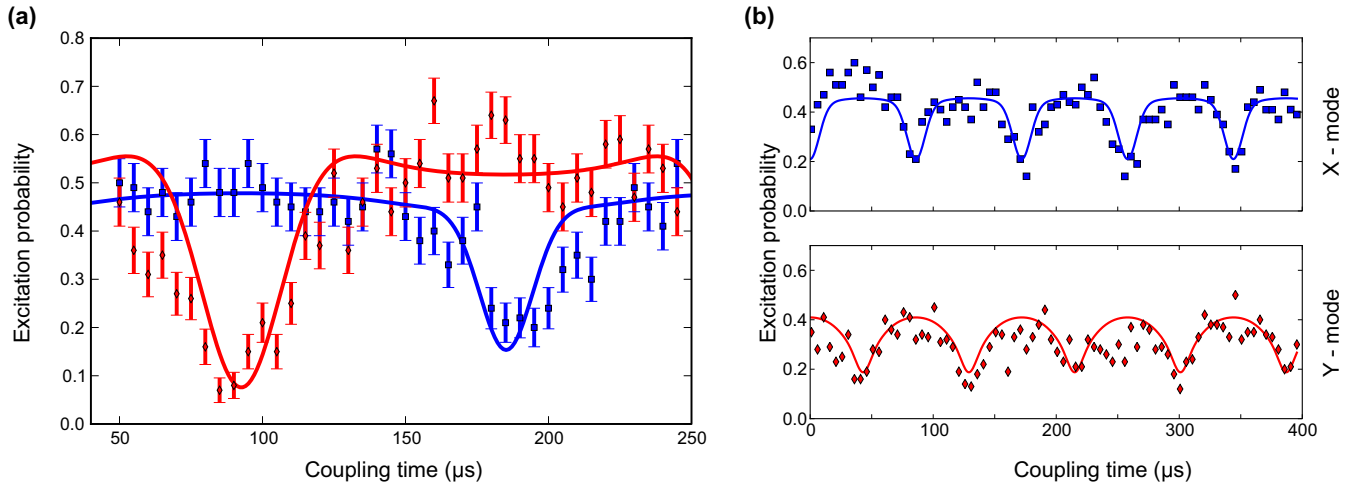

FIG. 4. (Color online) (a) Time evolution of the coupling dynamics illustrated by the excitation of the red sideband of the Z (blue squares) and X (red diamonds) mode. Initially, the Z mode is cooled close to its ground state at a mean phonon number of $\bar{n}_z \approx 0.2$ while the X mode is left at the Doppler temperature of $\bar{n}_x \approx 6$ quanta. After a coupling time of around 90 μs, the population of the two modes is swapped and thus the X mode is close to its ground state. Solid lines correspond to a numerical solution of the model with no free parameters. The initial X mode population and coupling frequencies were determined from sideband spectroscopy. Note that the coupling time does not start at zero, because the Blackman-shaped pulse is not adiabatic in this regime. (b) Red sideband excitation of the X (blue squares) and Y (red diamonds) modes. The X mode is initially cooled to a mean phonon number of $\bar{n}_x \approx 0.3$. Solid lines indicate a fit to a model where the initial Y mode population and Rabi frequency are adjusted. The out-of-phase oscillations between the X and Y red sideband excitations show the population oscillating between the two modes.

IV. COOLING WITHOUT DIRECT ACCESS

A. Application: Ground-state cooling

The parametric coupling technique we describe here provides a useful addition to the mostly optical toolbox in ion trapping physics. In particular, it enables cooling motional modes without accessing them by laser beam.

The basic principle involves performing laser cooling on a single, laser-accessible mode (the *primary mode*), followed by population swapping to transfer energy from a secondary, uncooled mode, into the primary mode. One implementation of this technique is to perform several cooling cycles on the primary mode and to insert a SWAP operation between each cycle. With the parametric interaction operated in this way, the primary mode provides a cold reservoir for the secondary mode. After each cycle of sideband cooling, the populations of the primary and secondary modes are swapped, eventually resulting in a state where both the primary and secondary modes are prepared close to their ground state. We call this method of cooling *interleaved cooling*, allowing us to prepare both modes close to their ground states. Interleaved cooling is particularly elegant for ground-state preparation because it is insensitive to errors in the SWAP operation. Even a somewhat imperfect SWAP operation will transfer a large fraction of the population between the two modes mode, where the population in the primary mode is then removed by optical cooling. Repetition of this process several times leads to significant reduction in the secondary mode population.

Interleaved cooling can prepare both modes close to their ground states when the heating processes on both modes are slower than the cooling rate on the primary mode. However, even if this condition is not satisfied, it is still possible to prepare the secondary mode close to its ground state. Here, we take advantage of the SWAP operations that can be performed much faster than the typical cooling processes on optical transitions, as one is not limited by the relatively weak coupling of the light to the ion's motion. Therefore, one can cool the primary mode and perform a *single* SWAP operation subsequently, resulting in a cool secondary mode but a hot primary mode. This method is applicable as long as the SWAP operation can be performed faster than any heating process on the secondary mode.

We have tested both of these cooling techniques, using the Z mode as the primary and the X mode as the secondary. In the case of interleaved cooling, we performed eight cycles of sideband cooling with a SWAP operation between each, whereas for the single SWAP cooling, the Z mode was cooled for 8 ms followed by a single SWAP. We tabulate the results detailed in Table I, showing that both simultaneous ground-state cooling

TABLE I. Cooling results for both interleaved and single SWAP cooling methods. The interleaved method is capable of preparing two motional modes of the ion close to the ground state, provided that the heating rate in both modes is sufficiently low (see text). That the single SWAP method is somewhat less effective than the interleaved method for ground-state preparation reflects the method's higher sensitivity to errors in the parametric resonance frequency and mode swapping time as compared to the interleaved scheme.

Method	$\bar{n}_z$	$\bar{n}_x$
Interleaved	0.13(2)	0.31(5)
Single SWAP	7(5)	0.7(2)

by interleaved cooling and single SWAP cooling are effective techniques for cooling.

B. Application: Heating rate of an inaccessible mode

A second way to use the parametric interaction is to probe the thermal occupation of an inaccessible mode. We show that a heating rate can be measured in a mode nearly orthogonal to the laser propagation direction.

The heating rate on a single mode can be accurately determined by a process of cooling the mode to an average excitation much smaller than one vibrational quantum and then probing the red and blue sideband excitations as a function of a variable waiting time after cooling [3]. However, this process relies on the ability to prepare the motional state to small mean phonon numbers, as well as on optical access to the secular sidebands to read out the mode occupation.

In our experiment, the Y mode lies nearly perpendicular to the plane of the trap, such that the projection of the laser onto this mode is about 9°—too small to use sideband cooling directly on the mode. Thus, in order to prepare the mode to small thermal occupation, we perform sideband cooling on the X mode and then a single SWAP operation to initialize the Y mode to a mean thermal occupation of less than a single quantum. To determine the heating rate, we analyze the mode temperature as discussed above after a variable waiting time.

Due to the fact that the laser is not completely orthogonal to the Y mode, the mode temperature can be analyzed directly on the secular sidebands corresponding to the Y secular sideband. However, this requires comparably long (exceeding 500 μs) optical excitation times, during which instabilities in the mode frequency cause systematic errors. Furthermore, the excitation time is not short compared to the heating processes, adding another systematic error. Therefore, a much cleaner approach is to again apply a SWAP operation between the X and Y modes to exchange their populations.

In order to verify that the second SWAP operation works as expected, we performed a heating rate experiment using both of the above techniques, with the heating time varied between 0 and 2 ms. The results of these experiments are shown in Fig. 5. The measurement using the direct analysis of the sideband infers a heating rate of 650(270) quanta/s whereas the measurement employing two SWAP operations yields 810(80) quanta/s. The smaller uncertainty from temperature of the Y mode via the X mode reflects the fact that the Rabi frequency on the X red sideband is considerably faster than that of the Y mode. This renders the temperature measurement much less sensitive to instabilities in the radial motional frequencies due to the reduced Fourier bandwidth of the applied pulses.

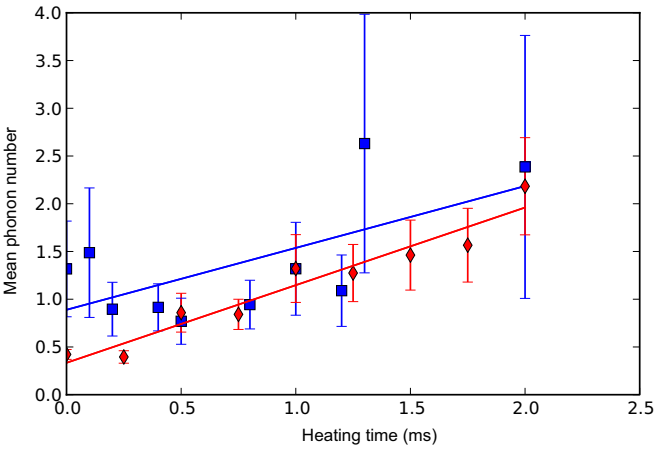

FIG. 5. (Color online) Mean phonon number as a function of heating time on the Y mode. The Y mode is prepared close to its ground state by cooling the X mode and swapping the motional states. Analysis of the motional state is either performed directly on the Y mode (blue squares) or by a second coupling operation and subsequent analysis on the X mode (red diamonds). The red (bottom) line corresponds to a heating rate of 810(80) quanta/s, while the blue (top) line corresponds to a heating rate of 650(270) quanta/s.

V. CONCLUSIONS

We have shown that inducing mode-mode coupling by means of a parametric drive can be readily applied to the case of trapped ions in surface electrode Paul traps. The presented method provides control of motional modes which lack direct optical access, reducing experimental design constraints. Both in surface science studies and in experiments aimed at coupling the motion of single ions to solid state systems [19–22], optical access to the modes of interest might be seriously compromised. Thus, we expect this parametric coupling technique to be useful in overcoming the related challenges of these experiments by allowing the experimenter to control and measure the temperature of optically inaccessible modes.

We also used the mode-mode coupling scheme to show ground-state cooling and a subsequent heating rate measurement on a mode that was not addressed optically. With heating rates sufficiently slow, the interleaved cooling scheme can be used to simultaneously prepare two modes close to their quantum mechanical ground state. Simultaneous cooling of several modes has been shown, for instance, in electromagnetically induced transparency cooling, but in that case the modes must be sufficiently close in frequency for cooling to be effective [23]. The interleaved cooling technique, however, can also be applied if the modes have very different frequencies.

It may also be possible to use this method to generate nonclassical motional states. Indeed, as we noted in Eq. (4), the system can be operated as a parametric amplifier, yielding two-mode squeezing [24]. Additionally, it may be possible to generate two-mode entanglement by ground-state-cooling two modes, performing coherent rotation on a single mode, and then applying the driving pulse for half of the swap time.

We expect that this method can be straightforwardly applied to couple the center-of-mass modes of a string of ions. It is less obvious that the coupling can also be extended to the other normal modes of the string. The fundamental requirement is that the coupling potential mixes the eigenmodes of the unperturbed potential, requiring sufficient variation of the coupling potential on the scale of the interion distance in

the string. Further investigation is needed to quantify the requirements for trap design enabling coupling of all modes in an ion string.

ACKNOWLEDGMENT

This work has been supported by AFOSR through the ARO Grant No. FA9550-11-1-0318.

[1] R. Blatt and D. Wineland, Nature (London) **453**, 1008 (2008).
[2] H. Häffner, C. F. Roos, and R. Blatt, Phys. Rep. **469**, 155 (2008).
[3] D. Leibfried, R. Blatt, C. Monroe, and D. Wineland, Rev. Mod. Phys. **75**, 281 (2003).
[4] T. Monz, P. Schindler, J. T. Barreiro, M. Chwalla, D. Nigg, W. A. Coish, M. Harlander, W. Hänsel, M. Hennrich, and R. Blatt, Phys. Rev. Lett. **106**, 130506 (2011).
[5] D. J. Wineland and H. G. Dehmelt, J. Appl. Phys. **46**, 919 (1975).
[6] L. S. Brown and G. Gabrielse, Rev. Mod. Phys. **58**, 233 (1986).
[7] E. A. Cornell, R. M. Weisskoff, K. R. Boyce, and D. E. Pritchard, Phys. Rev. A **41**, 312 (1990).
[8] D. Kielpinski, C. Monroe, and D. J. Wineland, Nature (London) **417**, 709 (2002).
[9] W. Paul, Rev. Mod. Phys. **62**, 531 (1990).
[10] H. G. Dehmelt, Adv. At. Mol. Phys. **3**, 53 (1968).
[11] D. M. Meekhof, C. Monroe, B. E. King, W. M. Itano, and D. J. Wineland, Phys. Rev. Lett. **76**, 1796 (1996).
[12] D. J. Wineland, C. Monroe, W. M. Itano, D. Leibfried, B. E. King, and D. M. Meekhof, J. Res. Natl. Inst. Stand. Technol. **103**, 259 (1998).
[13] H. G. Dehmelt, Bull. Am. Phys. Soc. **20**, 60 (1975).
[14] Q. A. Turchette, D. Kielpinski, B. E. King, D. Leibfried, D. M. Meekhof, C. J. Myatt, M. A. Rowe, C. A. Sackett, C. S. Wood, W. M. Itano, C. Monroe, and D. J. Wineland, Phys. Rev. A **61**, 063418 (2000).
[15] AVX X7R 47nF; Part No. W3H15C4738AT1F, showing a measured cutoff frequency of 300 kHz.
[16] D. Berkeland, J. Miller, J. Bergquist, W. Itano, and D. Wineland, J. Appl. Phys. **83**, 5025 (1998).
[17] F. J. Harris, Proc. IEEE **66**, 51 (1978).
[18] M. Riebe, K. Kim, P. Schindler, T. Monz, P. O. Schmidt, T. K. Körber, W. Hänsel, H. Häffner, C. F. Roos, and R. Blatt, Phys. Rev. Lett. **97**, 220407 (2006).
[19] N. Daniilidis, S. Gerber, G. Bolloten, M. Ramm, A. Ransford, E. Ulin-Avila, I. Talukdar, and H. Häffner, Phys. Rev. B **89**, 245435 (2014).
[20] N. Daniilidis, D. J. Gorman, L. Tian, and H. Häffner, New J. Phys. **15**, 073017 (2013).
[21] N. Daniilidis, T. Lee, R. Clark, S. Narayanan, and H. Häffner, J. Phys. B **42**, 154012 (2009).
[22] D. A. Hite, Y. Colombe, A. C. Wilson, K. R. Brown, U. Warring, R. Jördens, J. D. Jost, K. S. McKay, D. P. Pappas, D. Leibfried, and D. J. Wineland, Phys. Rev. Lett. **109**, 103001 (2012).
[23] C. F. Roos, D. Leibfried, A. Mundt, F. Schmidt-Kaler, J. Eschner, and R. Blatt, Phys. Rev. Lett. **85**, 5547 (2000).
[24] C. Gerry and P. Knight, *Introductory Quantum Optics* (Cambridge University Press, Cambridge, UK, 2004).